

Steric Effects in the Aerobic Oxidation of π -Allylnickel(II) Complexes with *N*-Heterocyclic Carbenes

Benjamin R. Dible and Matthew S. Sigman*

Department of Chemistry, University of Utah, Salt Lake City, Utah 84112

Received July 5, 2006

π -Allylchloro(NHC)nickel(II) complexes were synthesized and their reactions with O₂ were studied. Ligand steric effects were found to determine the difference between rapid oxidation of the allyl group to produce bis- μ -hydroxonickel complexes and no observable reaction. The ability of the metal–NHC bond to rotate correlates with the ability of the complex to react with O₂. In the limiting cases, conformationally restricted complexes are stable to O₂ and complexes with rapid Ni–NHC bond rotation react rapidly with O₂. Complexes with intermediate conformational flexibility were found to exhibit lesser reactivity with O₂. On the basis of the observed inertness of complexes with saddle-shaped ligands to O₂, we propose the adoption of a nonplanar geometry upon reaction with O₂ to be required. The issue of conformational flexibility versus rigidity is expected to directly impact the catalytic behavior of metal–NHC complexes.

Introduction

The emergence of *N*-heterocyclic carbenes (NHCs, see Figure 1) since Arduengo's seminal publication in 1991¹ has invigorated the catalysis field by providing a powerful complement to phosphine/arsine ligands for a wide array of reactions from olefin metathesis² to cross-coupling.^{3,4} Among the useful properties of NHCs is a pronounced stability to O₂, which makes them potent ligands for transition-metal-mediated aerobic oxidations.^{5–9}

It is widely believed that NHCs are stronger σ -donors than phosphines. Measurements of Tolman electronic parameters¹⁰ (TEP) by Crabtree¹¹ and Nolan¹² strongly support this

Table 1. Tolman Electronic Parameters (TEPs) for NHCs and Selected Phosphines

ligand	ν (cm ⁻¹)	ligand	ν (cm ⁻¹)
ICy ^a	2049.6	IBioxMe ₄ ^c	2054
tmly ^b	2050	P(^t Bu) ₃ ^d	2056.1
biy ^b	2051	PBu ₃ ^d	2060.3
IMes ^a	2050.7	PMe ₃ ^d	2064.1
SIMes ^a	2051.5	P(o-Tol) ₃ ^d	2066.6
IPr ^a	2051.5	PPh ₃ ^d	2068.9
SlIPr ^a	2052.2		

^a Nolan.¹² ^b Crabtree.¹¹ ^c Glorius.¹³ ^d Tolman.¹⁰

viewpoint (Table 1). What is striking about these measurements is how small the differences in TEP values are among reported NHCs, essentially falling within a 3 cm⁻¹ range (4.5 cm⁻¹ if IBioxMe₄ is included).¹³ On the other hand, TEP values for phosphines vary by more than 12 cm⁻¹. It should be noted that the TEP values reported by Crabtree¹¹ and Glorius¹³ were determined using iridium complexes. The relatively narrow range of TEP values for NHCs as compared to phosphines suggests that differences in the properties of metal–NHC complexes with varying NHCs are more likely to stem from steric effects.

To describe the steric effects of NHCs on nickel complexes, Nolan recently proposed to consider the fraction of the metal sphere occupied by the ligand: %*V*_{bur}.¹² Essentially, the larger the %*V*_{bur} value, the more steric pressure exerted

* To whom correspondence should be addressed. E-mail: sigman@chem.utah.edu.

- (1) Arduengo, A. J., III; Harlow, R. L.; Kline, M. *J. Am. Chem. Soc.* **1991**, *113*, 361–363.
- (2) Trnka, T. M.; Grubbs, R. H. *Acc. Chem. Res.* **2001**, *34*, 18–29.
- (3) Herrmann, W. A. *Angew. Chem., Int. Ed.* **2002**, *41*, 1290–1309.
- (4) Navarro, O.; Kelly, R. A., III; Nolan, S. P. *J. Am. Chem. Soc.* **2003**, *125*, 16194–16195.
- (5) Jensen, D. R.; Schultz, M. J.; Mueller, J. A.; Sigman, M. S. *Angew. Chem., Int. Ed.* **2003**, *42*, 3810–3813.
- (6) Jensen, D. R.; Sigman, M. S. *Org. Lett.* **2003**, *5*, 63–65.
- (7) Cornell, C. N.; Sigman, M. S. *J. Am. Chem. Soc.* **2005**, *127*, 2796–2797.
- (8) Schultz, M. J.; Hamilton, S. S.; Jensen, D. R.; Sigman, M. S. *J. Org. Chem.* **2005**, *70*, 3343–3352.
- (9) Sigman, M. S.; Jensen, D. R. *Acc. Chem. Res.* **2006**, *39*, 221–229.
- (10) Tolman, C. A. *Chem. Rev.* **1977**, *77*, 313–348.
- (11) Chianese, A. R.; Li, X.; Janzen, M. C.; Faller, J. W.; Crabtree, R. H. *Organometallics* **2003**, *22*, 1663–1667.
- (12) Dorta, R.; Stevens, E. D.; Scott, N. M.; Costabile, C.; Cavallo, L.; Hoff, C. D.; Nolan, S. P. *J. Am. Chem. Soc.* **2005**, *127*, 2485–2495.

- (13) Altenhoff, G.; Goddard, R.; Lehmann, C. W.; Glorius, F. *J. Am. Chem. Soc.* **2004**, *126*, 15195–15201.

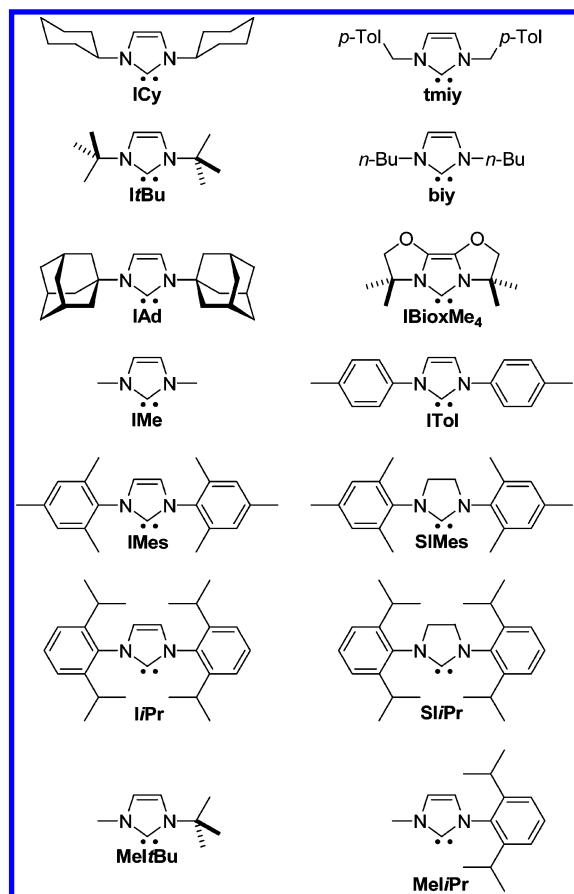


Figure 1. *N*-Heterocyclic Carbenes (NHCs) discussed in this manuscript.

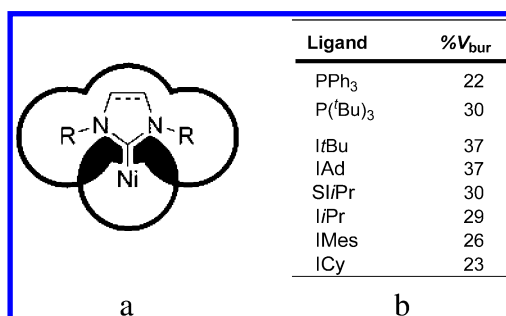
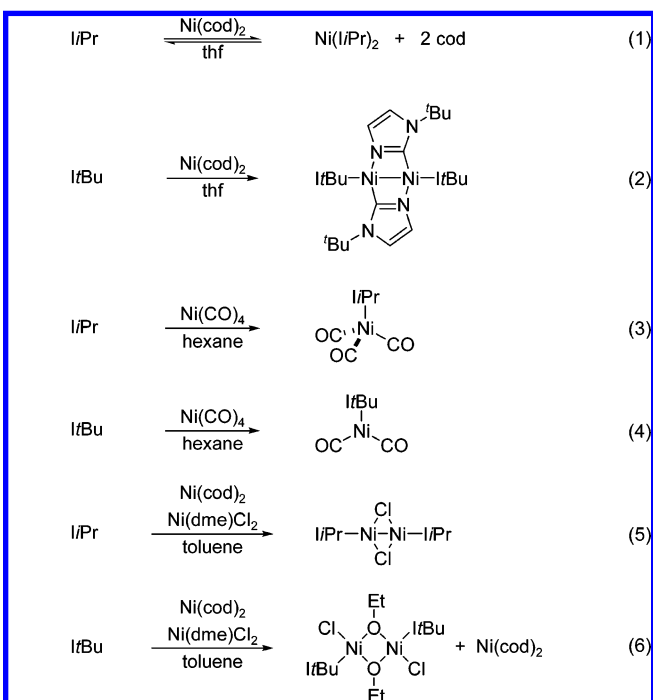


Figure 2. (a) Depiction of %*V*_{bur}, where the darkened area depicts the space filled about the nickel center by the ligand. (b) Values of %*V*_{bur} reported by Nolan.¹²

by the ligand. An illustration of %*V*_{bur} and the reported values for nickel are shown in Figure 2. Nolan has also proposed the use of %*V*_{bur} for palladium¹⁴ and ruthenium¹⁵ complexes with NHCs.

In the context of nickel–NHC systems, there are several documented examples of discrepancies in reactivity between *IPr* and *ItBu*. For example, the respective reactions of *IPr* and *ItBu* with various nickel sources have drastically different outcomes. The reaction of *IPr* with Ni(cod)₂ is reported to form Ni(*IPr*)₂ cleanly (eq 1),¹⁶ although it has also been

proposed to be a reversible reaction.¹⁷ In contrast, the reaction of *ItBu* with Ni(cod)₂ produces several fascinating products, but not Ni(*ItBu*)₂ (eq 2).¹⁸ In this case, %*V*_{bur} correlates with the results: the larger ligand fails to form a stable NiL₂ complex. The reaction of *IPr* with Ni(CO)₄ produces saturated, tetrahedral Ni(CO)₃(*IPr*) (eq 3) whereas the reaction of *ItBu* with Ni(CO)₄ produces unsaturated, trigonal Ni(CO)₂(*ItBu*) (eq 4).¹² This result is consistent with %*V*_{bur} in that the larger ligand leads to the formation of a less coordinated product. Since this report on %*V*_{bur} and NHC–nickel complexes appeared, our lab has reported a discrepancy between *IPr* and *ItBu* in the attempted synthesis of bis- μ -chloronickel(I) complexes. When a 1:1 mixture of Ni(cod)₂ and Ni(dme)Cl₂ is treated with 2 equiv of *IPr* in toluene, the desired bis- μ -chloronickel(I) complex is produced (eq 5). Treating the same mixture of nickel sources with 2 equiv of *ItBu* results in the formation of a bis- μ -ethoxonickel(II) complex, apparently due to an ethanol impurity in the Ni(dme)Cl₂ used (eq 6). It should be noted that the same bottle of Ni(dme)Cl₂ source was used for the reactions in eqs 5 and 6 and that the use of ethanol-free Ni(dme)Cl₂ prevented formation of the bis- μ -ethoxonickel(II) complex shown in eq 6.¹⁹ In this case, the ligand with the larger %*V*_{bur} value leads to the formation of a more-coordinated product. This result is not consistent with %*V*_{bur}.



To study this discrepancy in more detail, we harnessed the O₂ reactivity of π -allylchloro(NHC)nickel(II) complexes previously reported from our lab.²⁰ A number of additional complexes were prepared in order to evaluate steric effects

- (14) Viciu, M. S.; Navarro, O.; Germaneau, R. F.; Kelly, R. A., III; Sommer, W.; Marion, N.; Stevens, E. D.; Cavallo, L.; Nolan, S. P. *Organometallics* **2004**, *23*, 1629–1635.
- (15) Hillier, A. C.; Sommer, W. J.; Yong, B. S.; Petersen, J. L.; Cavallo, L.; Nolan, S. P. *Organometallics* **2003**, *22*, 4322–4326.
- (16) Böhm, V. P. W.; Gstöttmayr, C. W. K.; Weskamp, T.; Herrmann, W. A. *Angew. Chem., Int. Ed.* **2001**, *40*, 3387–3389.

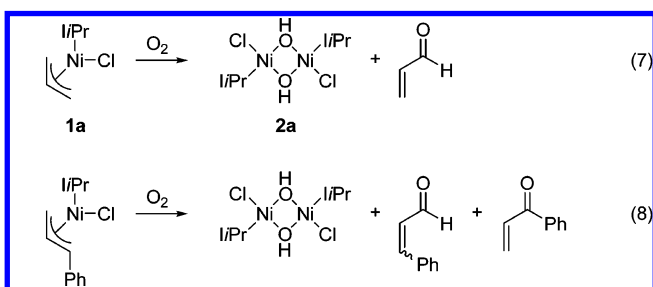
- (17) Louie, J.; Gibby, J. E.; Farnworth, M. V.; Tekavec, T. N. *J. Am. Chem. Soc.* **2002**, *124*, 15188–15189.
- (18) Caddick, S.; Cloke, F. G. N.; Hitchcock, P. B.; Lewis, A. K. d. K. *Angew. Chem., Int. Ed.* **2004**, *43*, 5824–5827.
- (19) Dible, B. R.; Sigman, M. S.; Arif, A. M. *Inorg. Chem.* **2005**, *44*, 3774–3776.
- (20) Dible, B. R.; Sigman, M. S. *J. Am. Chem. Soc.* **2003**, *125*, 872–873.

on this reaction. Herein, we present the results of this study, which strongly implicate sterics as the dominant factor affecting the O₂ reactivity of π -allylnickel complexes with NHCs and possibly the dominant factor affecting other nickel–NHC systems as well.

Results and Discussion

Synthesis of π -Allylchloro(NHC)nickel(II) Complexes. π -Allylchloro(NHC)nickel(II) complexes were synthesized via the one-pot procedure we reported previously for *IrPr*.²⁰ In this reaction, Ni(cod)₂ is oxidized by allyl chloride using 1,5-cyclooctadiene (cod) as the solvent. A solution of NHC in toluene is added to the resulting π -allylnickel(II) intermediate in a dropwise fashion to generate the desired π -allylchloro(NHC)nickel(II) product. This reaction proceeds in good to excellent yields, as shown in Table 2. The NHCs were isolated prior to use following the procedure developed by Arduengo,²¹ except in cases where the NHCs were not amenable to isolation. In those cases, the NHC was generated in situ and then added to the π -allylnickel(II) intermediate and the yields were substantially lower. As noted by Arduengo, the key to isolating NHCs is the avoidance of water, where sensitive NHC's seem to originate from more hygroscopic imidazolium salts. It is noteworthy that drying the precursor imidazolium salts via azeotropic distillation with toluene using a Dean–Stark trap is especially beneficial for IMes, ITol, and IMe.²¹

Reactions of π -Allylchloro(NHC)nickel(II) Complexes with O₂. In an earlier communication, we reported on the unusual reaction of π -allylchloro(*IrPr*)nickel(II) with O₂ (eqs 7 and 8).¹² In this reaction, a bis- μ -hydroxochloro(*IrPr*)nickel-



(II) dimer is produced and the allyl groups are oxidized and liberated as α,β -unsaturated carbonyl compounds. *IrPr* complex **1a** was found to react rapidly with oxygen in hexanes, benzene, toluene, and thf, with rates increasing in that series from hexanes to thf. However, complex **1a** is kinetically stable to O₂ in methylene chloride and 1,2-dichloroethane, with reaction times greater than 36 h. It should be noted that even the addition of small amounts of CH₂Cl₂ to benzene or THF (1:10 mixtures) prohibits oxidation, which may be due to competitive inhibition of O₂ binding by chlorinated solvents. The analogous *SIrPr* (**1b**) and IMes (**1c**) complexes behaved in a similar manner (Figure 3), with formation of purple products with λ_{max} (**1b**) = 492 nm and λ_{max} (**1c**) = 497 nm. These are consistent with

Table 2. Preparation of π -Allylchloro(NHC)Nickel(II) Complexes from Ni(cod)₂

	NHC	solvent	yield (%)
1a	<i>IrPr</i>	PhMe	99 ^a
1b	<i>SIrPr</i>	PhMe	99 ^a
1c	IMes	PhMe	98 ^a
1d	<i>IrBu</i>	PhMe	>99 ^a
1e	IAd	PhMe	98 ^a
1f	IBioxMe ₄	thf	74 ^b
1g	ICy	thf	51 ^b
1h	ITol	PhMe	63 ^a
1i	Mel <i>t</i> Bu	PhMe	56 ^b
1j	Mel <i>i</i> Pr	thf	47 ^b
1k	IMe	thf	53 ^{b,c}

^a Isolated NHC used. ^b NHC generated in situ. ^c Isolated (C₃H₅NiCl)₂ used.

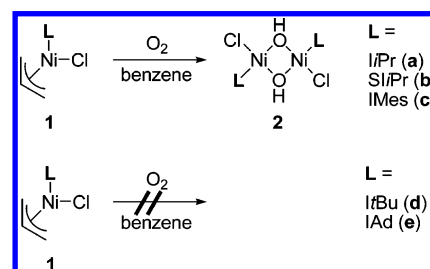


Figure 3. Reactions of π -allylchloro(NHC)nickel(II) complexes **1a–1e** with O₂.

the λ_{max} value of 500 nm previously reported for bis- μ -hydroxonickel(II) complex **2a**.²⁰ Attempts to isolate the putative bis- μ -hydroxonickel(II) products of the oxidation of **1b** or **1c** were unsuccessful because of decomposition of the products in solution. Even the previously reported, crystallographically characterized bis- μ -hydroxonickel(II) complex **2a** decomposes in solution. For this reason, discussion of the O₂ stability of π -allylchloro(NHC)nickel(II) complexes is based on consumption of the π -allylnickel complexes.

We next examined the *IrBu* (**1d**) and IAd (**1e**) analogues and were greatly surprised to find that they were stable to O₂, even when refluxed under an O₂ atmosphere in *d*₆-benzene. No new species were observed by ¹H NMR, nor was the formation of insoluble products observed. This contrasts markedly with the aforementioned complexes **1a–1c**, which oxidize in a matter of seconds at room temperature. This discrepancy was initially of unknown origin. The O₂-stable complexes of *IrBu* (**1d**) and IAd (**1e**) each have *N,N'*-dialkyl substituents, whereas the reactive complexes of *IrPr* (**1a**), *SIrPr* (**1b**), and IMes (**1c**) all have *N,N'*-diaryl substituents. It would be tempting to call this discrepancy an electronic effect, but the TEP value for IMes is 2050.7 and the TEP values for *N,N'*-dialkyl substituted NHC ligands ICy, tm_{iy}, and biy range from 2049.6 to 2051. These values strongly suggest that electronic effects are not the determining factor. Furthermore, one would expect that stronger σ -donors, ligands with smaller TEP values, would be more susceptible to oxidation if electronic effects were the sole determining factor. However, to disprove electronic effects

(21) Arduengo, A. J., III; Dias, H. V. R.; Harlow, R. L.; Kline, M. J. *Am. Chem. Soc.* **1992**, *114*, 5530–5534.

as the determining factor, we would require either a reactive non-aryl-substituted NHC or an inert aryl-substituted NHC.

The recent publications by Glorius on IBiox ligands¹³ inspired an attempt to prepare a complex with a constrained *ItBu* analogue. An examination of the crystal structure of IBioxMe₄–HOTf suggested that IBioxMe₄ would be ideal for this study. IBioxMe₄ complex **1f** was prepared and characterized crystallographically. As expected, IBioxMe₄ is less hindering than *ItBu*. Furthermore, IBioxMe₄ complex **1f** was found to oxidize rapidly when treated with O₂ in thf and slowly in benzene. The TEP value for IBioxMe₄ is 2054 cm^{−1}, which is slightly larger than those measured for *N,N'*-dialkyl NHC ligands. The observed instability of **1f** to O₂ suggested that the tipping point between O₂ stability and instability was close, which inspired the study of NHC ligands with smaller alkyl substituents or with fewer aryl substituents.

ICy complex (**1g**) and ITol complex (**1h**) were prepared for study with O₂. ICy complex **1g** was completely consumed within 5 s in oxygenated thf at 0 °C with concomitant formation of a purple species with $\lambda_{\text{max}} = 483$ nm. This successfully disproves that dialkyl-substituted NHCs always form O₂-stable complexes, which in turn refutes electronic effects as the sole determining factor. ITol complex **1h** was consumed in ca. 30 min under these conditions. It should be noted that *ItPr* complex **1a**, *SI**Pr* complex **1b**, and IMes complex **1c** were completely consumed within 5 s under these conditions.

When oxygenated benzene was used as the reaction solvent at room temperature instead of thf at 0 °C, ICy complex **1g** was consumed within 5 min. Under these conditions, *ItPr* complex **1a**, *SI**Pr* complex **1b**, and IMes complex **1c** were still consumed within 5 s. In stark contrast, ITol complex **1h** was not observed to form a bis- μ -hydroxonickel(II) complex under these conditions, instead undergoing a side reaction to produce *trans*-[ITol₂NiCl₂] (**3h**). Control experiments revealed that this reaction does not require O₂. Furthermore, this reaction has not been observed for any other complex presented herein.

Dynamic NMR Study of NHC Complexes. The complexes evaluated above can be divided into three groups: O₂ reactive (**1a**, **1b**, and **1c**), moderately O₂ reactive (**1g** and **1h**), and O₂ stable (**1d** and **1e**). Ligands for the O₂-reactive complexes have % *V*_{bur} values ranging from 26 to 30. Ligands for the O₂-stable complexes each have % *V*_{bur} values of 37. ICy, the ligand for moderately reactive complex **1g**, has a % *V*_{bur} value of 23. There is no simple correlation between O₂ reactivity and % *V*_{bur} values among complexes **1a–1h**. However, a lack of correlation with % *V*_{bur} does not disprove steric effects as the determining factor. % *V*_{bur} calculations use DFT-optimized geometries of the free ligands and then place the NHC ligands 2 Å from the metal center. The metal is then considered to be a sphere with a 3 Å radius, and % *V*_{bur} is defined as the percentage of that sphere occupied by the ligand. The inherent assumption in this model is that the ligand has a static conformation, but the metal–ligand bond freely rotates. Otherwise, treating the non-NHC portion of the complex as a sphere would be an invalid assumption.

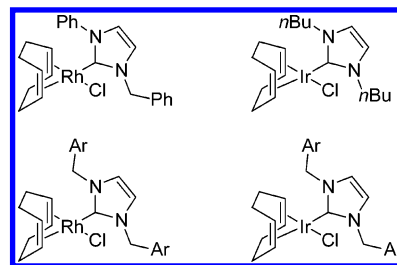


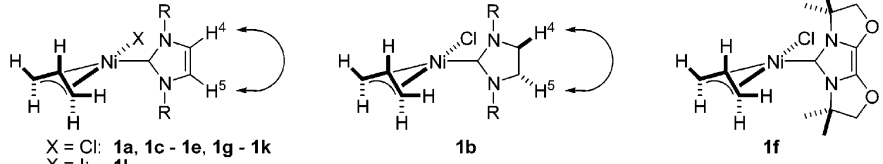
Figure 4. Selected NHC complexes reported to have hindered metal–NHC bond rotation.

If these conditions are not met, then the model should fail. To consider this possibility, we examined complexes **1a–1h** by dynamic ¹H NMR.

Crabtree reported and discussed several NHC complexes of rhodium and iridium that exhibited hindered rotation about the metal–carbene bond.¹¹ To summarize, square-planar iridium and rhodium complexes of NHCs exhibited fluxional or even fixed metal–NHC bond rotation on the NMR time scale at room temperature (Figure 4). In these cases, inhibited rotations were largely observable because of AB or ABXY splitting on the α -methylene protons on the *N*-substituents. Unfortunately, many of the NHCs and complexes used in catalysis lack spectroscopic handles to probe for inhibited metal–NHC rotation. As a consequence, the ability/inability of an NHC to rotate in a given complex seems to be given little consideration in terms of implications for catalysis. In our case, the planar chirality of η^3 -allyl complexes facilitates such observations.

The protons located on C4 and C5 of imidazol-2-ylidenes (backbone protons) are useful for purposes of examining metal–NHC rotation. In complexes that have slow metal–NHC rotation on the NMR time scale, these protons are nonequivalent and resolve as a pair of doublets. In complexes with freely rotating metal–NHC bonds, they are equivalent and appear as a singlet. Furthermore, these protons essentially account for the only signals observed between 5.5 and 7 ppm in η^3 -allylnickel(II) complexes. We have examined Ni–NHC rotations in η^3 -allylnickel(II) complexes by variable-temperature NMR, and the results are quite striking (Figure 5).

ItPr complex **1a**, *SI**Pr* complex **1b**, and IMes complex **1c** all exhibit rapid rotation on the NMR time scale. *ItBu* complex **1d** and IAd complex **1e** each exhibit no exchange on the NMR time scale, even at 80 °C. ICy complex **1g** and ITol complex **1h** each exhibit intermediate exchange on the NMR time scale. Backbone proton coalescence was observed at 45 °C for ICy complex **1g** and at 35 °C for ITol complex **1h**. From the coalescence data, it was possible to calculate ΔG_e^\ddagger values of 15.7 kcal/mol for ICy complex **1g** and 15.3 kcal/mol for ITol complex **1h**. To summarize: O₂-reactive complexes exhibit rapid Ni–NHC bond rotation, moderately O₂-reactive complexes exhibit slower Ni–NHC bond rotation, and O₂-stable complexes do not exhibit observable Ni–NHC bond rotation. It should be noted that the observed relative rates of rotation do not correlate with % *V*_{bur}. *ItBu* (% *V*_{bur} = 37) complex **1d** and IAd (% *V*_{bur} = 37) complex **1e** do not exhibit Ni–NHC bond rotation. *ItPr* (% *V*_{bur} = 29) complex **1a**, *SI**Pr* (% *V*_{bur} = 30) complex **1b**, and IMes



X = Cl: **1a**, **1c** - **1e**, **1g** - **1k**
X = I: **1l**

NHC	<i>d</i> ₆ -Benzene		Lifetime under O ₂			Product λ _{max} (solvent)
	H ⁴ -H ⁵ coalescence?	ΔG ₀ [‡] (kcal/mol)	C ₆ D ₆ ^a	thf ^b	CH ₂ Cl ₂ ^c	
I <i>i</i> Pr (1a)	< 20 °C	n.d.	< 5 sec	< 5 sec	~ 36h ^d	500nm (thf, PhMe)
SI <i>i</i> Pr (1b)	< 20 °C	n.d.	< 5 sec	< 5 sec	~ 12h ^d	492nm (PhMe)
IMes (1c)	< 20 °C	n.d.	< 5 sec	< 5 sec	~ 24h	497nm (PhMe)
I <i>t</i> Bu (1d)	> 80 °C	n.d. ^e	> 48h	> 48h	> 48h ^d	No Reaction
IAd (1e)	> 80 °C	n.d. ^e	> 48h	> 48h	> 48h ^d	No Reaction
IBioxMe ₄ (1f)	N / A	20.0 ^f	> 3h	< 5 sec	~ 12h ^d	488nm (thf)
ICy (1g)	~ 45 °C	15.7	< 5 min	< 5 sec	~ 10h ^d	483nm (thf)
ITol (1h)	~ 35 °C	15.3	> 3h ^d	~ 30 min	> 24h ^d	498nm (thf)
Me <i>i</i> Bu (1i)			> 3h	< 5 min	> 18h ^d	497nm (thf)
Me <i>i</i> Pr (1j)	< 20 °C	n.d.	< 5 sec	< 5 sec	~ 8h ^d	496nm (PhMe)
IMe (1k)	< 20 °C	n.d.	< 5 sec ^d	< 5 sec ^d	< 1h ^d	No λ _{max} in visible region
Me <i>i</i> Bu (1l)	> 80 °C	n.d. ^e	> 48h	~ 5h ^{d,h}	> 48h ^d	No Reaction

Notes: a) 3 - 6 mg/mL, rt. b) 0.5 - 1.3 mg/mL, 0 °C. c) 2.0 - 4.0 mg/mL, rt. d) no bis-μ-OH product obsd. e) no peak-broadening observed. f) Determined by methyl peak-broadening above 55 °C. g) no peak-broadening observed at T ≤ 62 °C. h) 1 mg/mL, rt.

Figure 5. Comparison of nickel–NHC bond rotations as observed by dynamic ¹H NMR (300 MHz) with O₂ stability.

(% *V*_{bur} = 26) complex **1c** each exhibit rapid Ni–NHC bond rotation. On the other hand, ICy (% *V*_{bur} = 23) complex **1g** exhibits intermediate Ni–NHC bond rotation, yet has a smaller % *V*_{bur} value. While in review, a manuscript detailing a study on dynamic NMR of π-allylnickel(II) complexes with IME was published, see: Silva, L. C.; Gomes, P. T.; Veiros, L. F.; Pascu, S. I.; Duarte, M. T.; Namorado, S.; Ascenso, J. R.; Dias, A. R. *Organometallics* **2006**, 25, 4391–4403.

It is worth noting that there is some evidence of inhibited rotation in related π-allylchloro(NHC)palladium(II) complexes. The NHC backbone protons in the I*t*Bu complex are reported as a pair of doublets in CDCl₃ by Faller and Sarantopoulos.²² However, the I*t*Bu complex is reported to have a single backbone peak in *d*₆-benzene by Viciu, Nolan, et al. The IAd complex is reported to have a doublet of doublets for the backbone peak in *d*₆-benzene in the same report.¹⁴ It appears that metal–NHC bond rotation is less sensitive to the nature of the NHC for palladium, possibly because of the slightly longer palladium(II)–NHC bonds of 2.03–2.06 Å¹⁴ compared to 1.90–1.93 Å for nickel(II).

Crystallographic Study. The crystal structures of **1a**²⁰ and **1d**^{12,23} were compared in order to develop a hypothesis as to why **1a** oxidizes and **1d** does not and to rationalize the observed correlation between Ni–NHC bond rotation and

O₂ reactivity (Tables 3 and 4). Notably, the steric bulk of the *t*-butyl groups in I*t*Bu is concentrated in the empty axial sites above and below the square plane of complex **1d** (Figure 6). On the other hand, the steric bulk of the isopropyl groups in I*i*Pr is more distributed in complex **1a**. These structural observations are consistent with the lack of observable Ni–I*t*Bu bond rotation in that the localized out of plane steric bulk of the *t*-butyl groups would be expected to cause a prohibitive activation barrier to rotation about that bond.

Incidentally, the blockage of the empty axial sites in I*t*Bu complex **1d** may be the source of O₂ stability. Prior mechanistic studies on the reaction of **1a** with O₂ indicate saturation kinetics with respect to **1a** and O₂.²⁰ The saturation behavior is consistent with the reversible formation of a reactive intermediate from **1a** and/or O₂, followed by rate-limiting decomposition of that intermediate. If the reactive intermediate in this oxidation is a nonplanar O₂ adduct, such as a superoxonickel(III) complex, then an available axial site would be required for oxidation to occur. Such intermediates have been proposed for observed aerobic ligand oxidations in nickel(II) complexes with dioxopentaazamacrocycles^{24–26} and with cyclotetrapeptides.²⁷ If this is the case, then Ni–

(22) Faller, J. W.; Sarantopoulos, N. *Organometallics* **2004**, 23, 2179–2185.

(23) We independently crystallized complex **1d** and present our data here.

(24) Chen, D.; Motekaitis, R. J.; Martell, A. E. *Inorg. Chem.* **1991**, 30, 1396–1402.

(25) Chen, D.; Martell, A. E. *J. Am. Chem. Soc.* **1990**, 112, 9411–9412.

(26) Cheng, C.-C.; Gulia, J.; Rokita, S. E.; Burrows, C. J. *J. Mol. Catal. A: Chem.* **1996**, 113, 379–391.

(27) Haas, K.; Dialer, H.; Piotrowski, H.; Schapp, J.; Beck, W. *Angew. Chem., Int. Ed.* **2002**, 41, 1879–1881.

Table 3. X-ray Diffraction Data Collection Parameters for Crystal Structures Discussed

	1a	1d	1f	1l
empirical formula	C ₃₀ H ₄₁ N ₂ Ni	C ₁₄ H ₂₅ ClN ₂ Ni	C _{17.5} H ₂₅ ClN ₂ NiO ₂	C ₁₁ H ₁₉ IN ₂ Ni
fw	523.81	315.52	389.55	364.89
<i>T</i> (K)	150(1)	150(1)	150(1)	150(1)
wavelength (Å)	0.71073	0.71073	0.71073	0.71073
cryst syst	monoclinic	orthorhombic	monoclinic	monoclinic
space group	<i>P</i> 2 ₁ / <i>c</i>	<i>Pna</i> 2 ₁	<i>P</i> 2 ₁ / <i>c</i>	<i>P</i> 2 ₁ / <i>c</i>
<i>a</i> (Å)	12.4456(2)	10.9968(3)	12.5757(4)	8.9469(3)
<i>b</i> (Å)	14.6922(2)	9.6424(3)	10.2031(2)	11.6836(3)
<i>c</i> (Å)	16.5225(3)	14.3616(2)	15.6864(4)	13.5112(4)
β (deg)	103.7751(6)	90	113.6613(10)	107.2586(13)
<i>V</i> (Å ³)	2934.30(8)	1522.84(7)	1843.54(8)	1348.76(7)
<i>Z</i>	4	4	4	4
ρ (g/cm ³)	1.186	1.376	1.404	1.797
μ (mm)	0.771	1.435	1.208	3.700
R1, wR2 (<i>I</i> > 2 σ (<i>I</i>))	0.0338, 0.0792	0.0240, 0.0521	0.0398, 0.0971	0.0375, 0.0957
GOF	1.018	1.054	1.047	1.058

Table 4. Selected Distances (Å) and Angles (deg) for π -Allylnickel–NHC Complexes

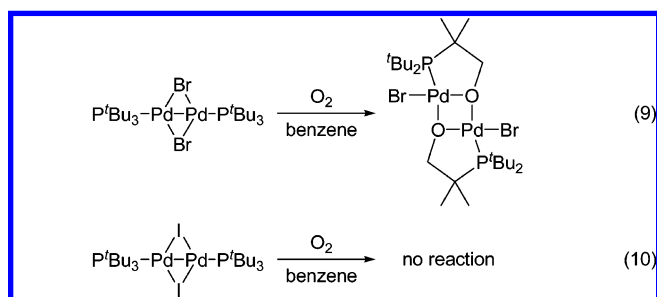
	1a	1d	1f	1l
Ni–C(carbene)	1.9025(16)	1.9290(18)	1.902(2)	1.909(4)
Ni–Cl (Ni–I for 1l)	2.1862(5)	2.2319(7)	2.2108(7)	2.5241(6)
Ni–C(allyl, cis to carbene)	1.981(2)	1.998(2)	2.004(3)	1.994(5)
Ni–C(allyl, internal)	1.972(2)	1.982(2)	2.000(4)	2.005(6)
Ni–C(allyl, trans to carbene)	2.056(2)	2.056(2)	2.056(3)	2.067(5)
C(carbene)–Ni–Cl (–I for 1l)	94.85(5)	97.91(6)	98.79(7)	95.31(11)
C(carbene)–Ni–C(allyl, cis)	98.21(8)	95.81(10)	93.85(10)	95.95(19)
C(carbene)–Ni–C(allyl, trans)	169.50(9)	167.37(11)	165.34(13)	168.86(19)
C(allyl, cis)–Ni–C(allyl, trans)	72.68(10)	72.76(12)	72.26(13)	73.2(2)

NHC bond rotation is simply a mechanism to open an axial site for O₂ binding. Perhaps other conformational changes could also permit O₂ binding. Both ICy complex **1g** and ITol complex **1h** exhibit slower Ni–NHC bond rotations than complexes **1a–1c** as well as reduced rates of oxidation. In both ICy complex **1g** and ITol complex **1h**, the barrier to rotation is between 15 and 16 kcal/mol. If Ni–NHC bond rotation is rate-limiting, then these two complexes should oxidize with similar rates. This is not the case. ICy complex **1g** reacts with O₂ faster than ITol complex **1h** does in either thf or benzene. If axial binding of O₂ is operative, then this discrepancy could stem from a requirement for both cyclohexyl groups to adopt a conformation oriented away from the square plane for rotation to occur, but with only one cyclohexyl group having to rotate away for oxidation. ITol complex **1g**, on the other hand, exhibits rapid *N*-aryl rotation, as observed by ¹H NMR, which would rotate the aryl groups through a conformation where the *p*-tolyl group is parallel to the imidazol-2-ylidene. In this conformation, the axial site on that face of the square plane would be blocked. It should be noted that *N*-aryl rotation was not observed for any other aryl-substituted ligand discussed herein (Figure 7). This explanation is internally consistent, but would benefit greatly from study of a complex that is incapable of nickel–NHC bond rotation yet has an open axial site. For this reason, an alternate ligand was devised.

It was envisioned that a nonsymmetrical NHC ligand with a large group on one side and a small group on the other could permit O₂ binding on one face of the square plane and block Ni–NHC rotation from steric interactions with the large group on the other face. A methyl group was considered to be the ideal small group and a *t*-butyl group to be the simplest large group. However, it was first

necessary to verify that *N*-methyl substituents would not interfere with O₂ reactivity. For this reason, Me*l*Pr complex **1j** and IMe complex **1k** were prepared and evaluated. In each case, rapid reaction with O₂ was observed, although there was no spectroscopic evidence for a bis(μ -hydroxo)nickel(II) product in the case of IMe complex **1k**.

Me*l*Bu complex **1i** was synthesized and characterized. The related iodo complex with Me*l*Bu, complex **1l**, was also prepared and studied via single-crystal X-ray diffraction. In each complex, Ni–NHC bond rotation was not observed by NMR, even at 80 °C. Chloro complex **1i** was found to react with O₂, albeit at slower rates than complexes **1a–1c**. On the other hand, iodo complex **1l** exhibited stability to O₂ comparable to that of *l*Tol complex **1d**. This was an unexpected development, but the substitution of iodine for another halogen was found to interrupt O₂ reactivity in a palladium(I) system (eqs 9 and 10),²⁸ so this phenomenon is not unique to nickel–O₂ chemistry.



Control Experiments. A notable alternative hypothesis for the pathway by which allylic oxidation occurs is via

(28) Durá-Vilá, V.; Mingos, D. M. P.; Vilar, R.; White, A. J. P.; Williams, D. J. *Chem. Commun.* **2000**, 1525–1526.

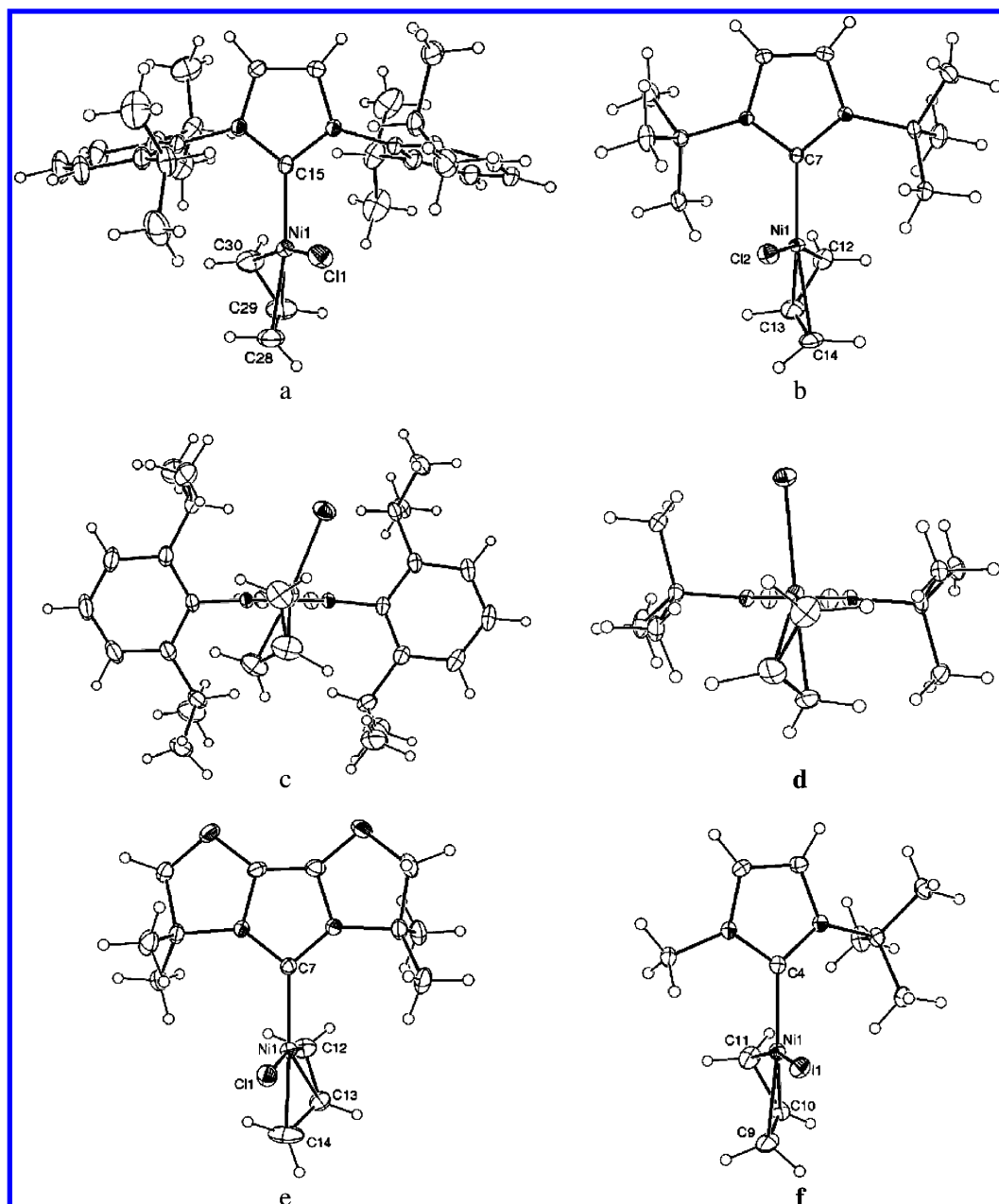
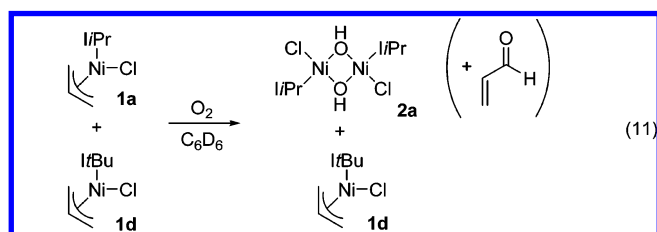


Figure 6. ORTEPs of (a) IPr complex **1a**, (b) IrtBu complex **1d**, (c) IPr complex **1a** viewed down the Ni–NHC bond, (d) IrtBu complex **1d** viewed down the Ni–NHC bond, (e) IBioxMe₄ complex **1f**, and (f) MeIrtBu complex **1i**.

autocatalysis. In this case, the difference between O₂-stable and O₂-reactive complexes could simply arise from the ability of a given complex to form a competent oxidation catalyst. This hypothesis was tested by treating a mixed solution of IPr complex **1a** and IrtBu complex **1d** in *d*₆-benzene with O₂. This resulted in the rapid, complete conversion of IPr complex **1a** into bis- μ -hydroxonickel(II) complex **2a** and acrolein with no change to IrtBu complex **1d** (eq 11). This

result does not disprove the possibility of such an autocatalytic mechanism, but it emphasizes that IrtBu complex **1d** is essentially inert to aerobic oxidation, regardless of whether the pathway is intermolecular or intramolecular, autocatalytic or not.

To probe the possibility of trace impurities promoting the reaction, we undertook a series of experiments with MeIrtBu complex **1i**. Complex **1i** was selected for study because it is the most O₂-resistant complex for which the formation of a bis- μ -hydroxonickel(II) species has been confirmed via visible spectroscopy. Samples of **1i** in thf were exposed to O₂ in the presence of the following additives: potassium *tert*-butoxide, Ni(cod)₂, and bis- η^3 -allylnickel chloride. Each of these three compounds is used at some stage within the synthesis of the complexes. The samples of **1i** were found



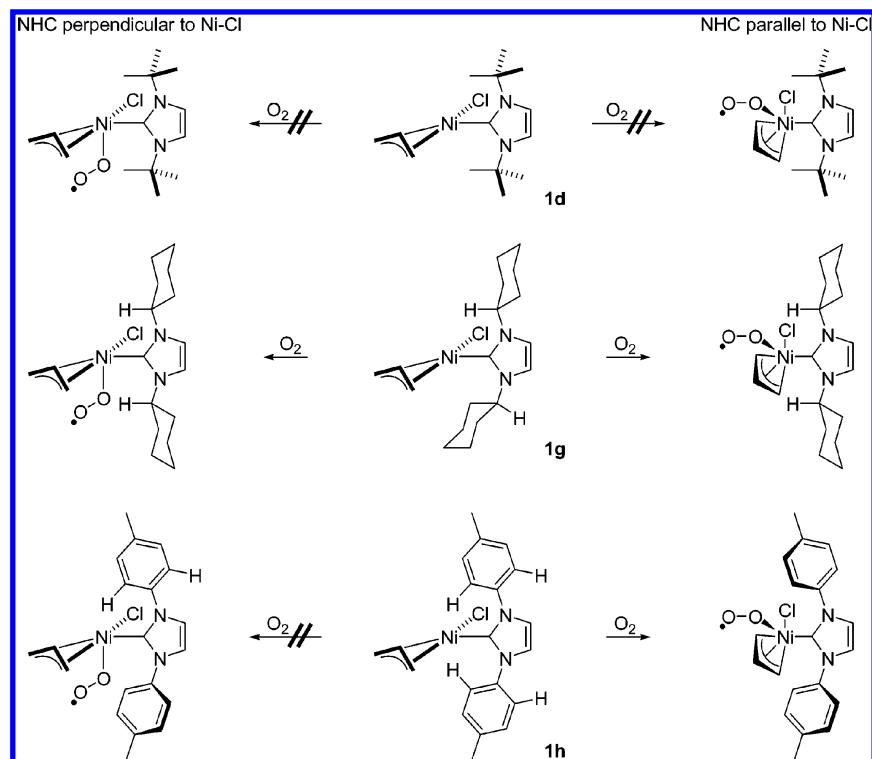


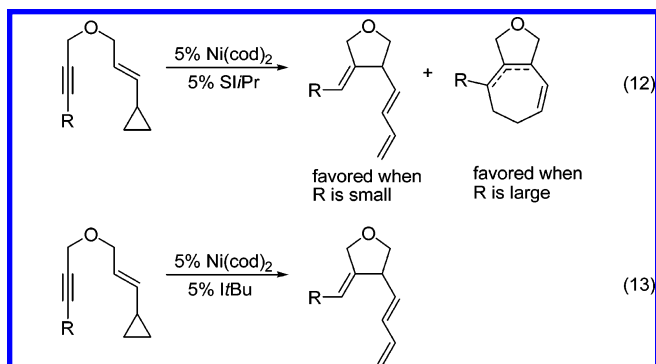
Figure 7. Putative nickel–NHC conformation effects on O_2 reactivity.

to decompose at the same rate as the additive-free control sample. A final control experiment was performed to determine the role of thf quality in O_2 reactivity. A sample of dry, distilled thf was sparged with O_2 for 15 min and subsequently heated to an incipient boil under an O_2 atmosphere. After cooling, a sample of **1i** in thf was added to the preoxygenated thf. Once again, no deviation from the control experiment was observed, casting doubt on the possibility that thf–peroxide formation is operative in the enhanced reactivity in thf.

Structural Implications

The fact that the more geometrically constrained complexes are not capable of reaction with O_2 in the same manifold suggests that reaction with O_2 requires a substantial geometric change about the metal. It is possible that reaction with O_2 requires the adoption of tetrahedral or a five-coordinate geometry to proceed, which would be consistent with the observed correlation between geometric constraint and inertness to O_2 (Figure 8). Formation of a tetrahedral O_2 adduct of **1a**, **1b**, or **1c** is consistent with observed tetrahedral $\text{Ni}(\text{CO})_3\text{-(NHC)}$ complexes of **1a**, **1b**, or **1c**.¹² However, **1g** also forms a tetrahedral $\text{Ni}(\text{CO})_3\text{-(NHC)}$ complex, yet **1g** is less reactive with O_2 . Facile metal–NHC bond rotation also does not appear to be required in cases where other mechanisms for opening space about the metal exist, such as a conformational change in a cyclohexyl group in **1g** or the presence of a more open face in **1i**. With these observations in mind, the most likely O_2 adduct is square pyramidal, although a bipyramidal geometry is also feasible.

The ability or inability to adopt a nonplanar geometry is almost certainly a relevant factor in nickel–NHC catalyzed processes. The imidazol-2-ylidene ligands that block axial space above and below the square plane exert the least steric pressure within the square plane. A recent report on Ni–NHC catalyzed cyclizations of cyclopropen-ynes by Zuo and Louie²⁹ is consistent with this quandary. When **SIPr** is used as the ligand, the distribution of products is dependent on the size of the alkyne substituent (eq 12). When **ItBu** is used, the only product observed is the product preferred for small alkyne substituents in the **SIPr** system (eq 13). This could be attributed to the less-crowded environment within the square-plane induced by **ItBu**, if one considers that **ItBu** is a saddle-shaped ligand. This would allow for more facile β -hydride elimination.



Conclusions

A series of π -allylchloro(NHC)nickel(II) complexes with varying NHCs have been prepared. These complexes are

(29) Zuo, G.; Louie, J. *J. Am. Chem. Soc.* **2005**, *127*, 5798–5799.

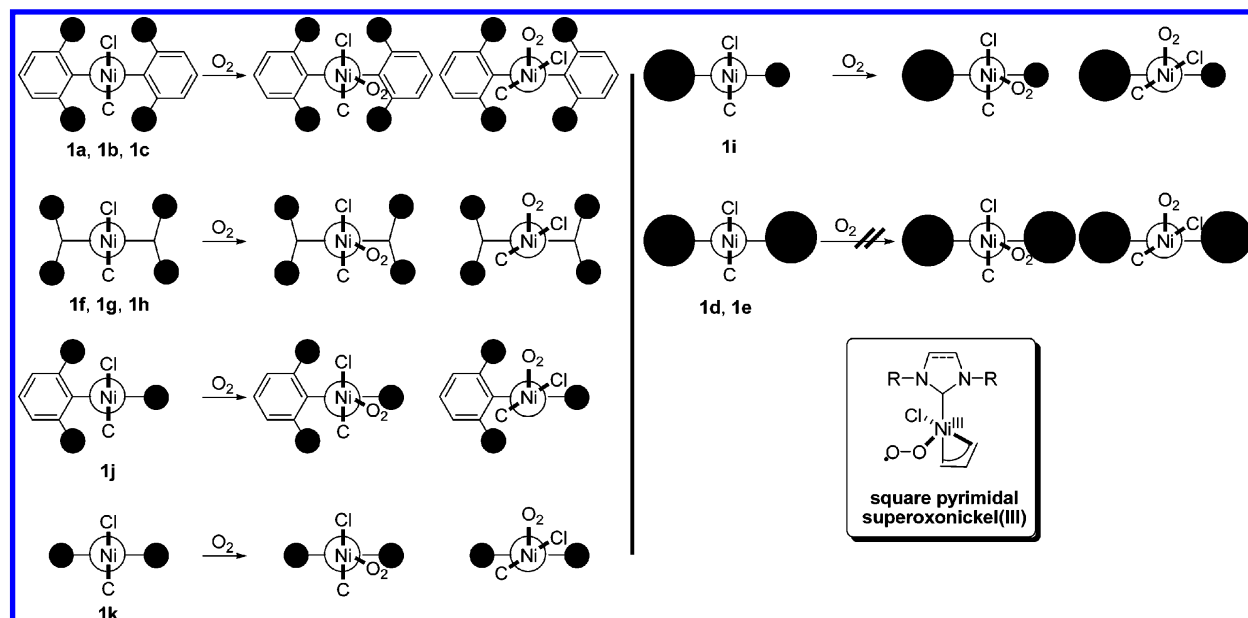


Figure 8. Newman projections of nonplanar O_2 adducts.

found to have a strong ligand dependence in terms of their ability to react with O_2 . The ligand dependence does not correlate with Tolman electronic parameters;^{12,13} therefore, electronic effects are not the determining factor. The ligand dependence also does not correlate with % V_{bur} .¹² However, it is notable that complexes resulting from ligands capable of blocking one or both of the empty axial sites above and below the square plane are inert to O_2 . Likewise, the ligand dependence strongly correlates with conformational freedom about the nickel–NHC bond: complexes with free rotation react with O_2 , complexes with restricted rotation do not react with O_2 , and complexes with intermediate conformational freedom exhibit intermediate reactivity. This correlation is consistent with a mechanism requiring the adoption of a nonplanar geometry about the metal as a requirement for reaction with O_2 . Furthermore, it has been demonstrated that an O_2 -reactive complex will not promote the reaction of an inert complex with O_2 .

Conformational restriction about metal–NHC bonds is relevant to catalysis and should be considered in terms of catalyst design and in the rationalization of observed patterns of reactivity. As in the case of cyclopropen-yn cyclization,²⁹ a conformationally restricted ligand may be advantageous. A monodentate ligand with a lesser volume within the square plane seems more likely to promote β -hydride elimination. Whether such a property is advantageous or problematic depends on the intended outcome, which is ample reason to consider the desired properties of an NHC-based catalyst carefully.

Experimental Section

General. Unless otherwise noted, all manipulations were carried out under an inert atmosphere using Schlenk techniques or in a VAC M0–40 glovebox. Glassware was oven- or flame-dried prior to use. Toluene, hexanes, and benzene were purified via passage through activated alumina columns and subsequently degassed under a vacuum. Tetrahydrofuran (thf) was purified by distillation

from sodium/benzophenone and subsequently degassed under a vacuum. Deuterated benzene and methylene chloride were dried using activated alumina and degassed via freeze–pump–thaw prior to use. Deuterated thf was purchased from Cambridge Isotope Laboratories and used as received. $Ni(\text{cod})_2$ was purchased from Strem and used as received. Allyl chloride was purified by distillation from CaCl_2 and degassed via freeze–pump–thaw. Allyl–($\text{I}i\text{Pr}$) $NiCl$ (**1a**),²⁰ $\text{SI}i\text{Pr}$, IMes ,²¹ IrBu , IAd , ICy , ITol ,²¹ IME ,²¹ and $\text{IBioxMe}_4\text{–HOTf}$ ¹³ were prepared as described in the literature. NMR spectra were collected on a Varian VXL-300 or on a Varian Unity-300. IR spectra were collected with a Mattson Satellite FTIR. Visible spectra were collected with an SI Photonics 440 series spectrophotometer equipped with a fiber-optic dip probe. Crystal structures were solved by Dr. Atta M. Arif. Mass Spectra were collected with a Finnigan MAT95 mass spectrometer by Dr. Elliot M. Rachlin. Elemental analyses were performed by Desert Analytics, Tucson, AZ.

Allyl(SI*i*Pr) $NiCl$ (1b**).** $Ni(\text{cod})_2$ (102 mg, 0.37 mmol) was suspended in cod (ca. 400 mg) in a scintillation vial. Allyl chloride (28 mg, 0.37 mmol) was then added dropwise to this suspension while the vial was swirled. A solution of $\text{SI}i\text{Pr}$ (145 mg, 0.37 mmol) in toluene (2-mL) was then added. Residual $\text{SI}i\text{Pr}$ was then transferred with toluene rinses (2×1 mL). The vial was swirled by hand until the mixture became homogeneous (ca. 3 min). The reaction mixture was then concentrated to dryness under a vacuum to yield the product as an orange solid (194 mg, 99% yield).

^1H NMR (300 MHz, C_6D_6): δ 0.82 (d, $J = 13$ Hz, 1H, allyl- H), 1.14 (t, $J = 7.2$ Hz, 12H, CHMe_2), 1.48 (d, $J = 6.4$ Hz, 6H, CHMe_2), 1.54 (d, $J = 6.1$ Hz, 6H, CHMe_2), 2.32 (d, $J = 6.1$ Hz, 1H, allyl- H), 2.45 (d, $J = 14$ Hz, 1H, allyl- H), 3.35 (d, $J = 6.3$ Hz, 1H, allyl- H), 3.54–3.44 (br s, 6H, overlapping $\text{RNCH}_2\text{CH}_2\text{–NR}$ and CHMe_2), 3.76 (m, 2H, CHMe_2), 4.45 (sept, $J = 6.8$ Hz, 1H, allyl- H), 7.1–7.2 (m, 6H, Ar- H). ^{13}C NMR $\{^1\text{H}\}$ (75 MHz, C_6D_6): δ 24.04, 24.30, 27.13, 27.215, 29.10, 44.25, 54.21, 71.72, 108.40, 124.94, 129.81, 137.24, 218.41. IR (KBr): 3070(w), 3056(w), 2958(s), 2868(s), 1475(m), 1446(s), 1419(s), 1266(s), 1239(m), 1054(m), 903(m), 801(m), 756(m), 424(w), 414(w). HRMS (EI) m/z : (M)⁺ calcd, 524.2490; obsd, 524.2484.

Allyl(IMes) $NiCl$ (1c**).** $Ni(\text{cod})_2$ (177 mg, 0.64 mmol) was suspended in cod (ca. 900 mg) in a scintillation vial. Allyl chloride

(49 mg, 0.64 mmol) was then added dropwise to this suspension while the vial was swirled. A solution of IMes (196 mg, 0.46 mmol) in toluene (2 mL) was then added. The residual IMes was transferred with toluene rinses (2×1 mL). The vial was swirled by hand until the mixture became homogeneous (ca. 3 min). The reaction mixture was then concentrated to dryness under a vacuum to yield the product as an orange solid (277 mg, 98% yield).

^1H NMR (300 MHz, C_6D_6): δ 1.18 (d, 1H, $J = 13$ Hz, allyl-*H*), 2.09 (s, 7H, Ar-*Me*), 2.15 (s, 6H, Ar-*Me*), 2.32 (s, 6H, Ar-*Me*), 2.46 (d, $J = 14$ Hz, 1H, allyl-*H*), 3.31 (d, $J = 6.8$ Hz, 1H, allyl-*H*), 4.63 (sept, $J = 6.8$ Hz, 1H, allyl-*H*), 6.16 (s, 2H, RNCHCHNR), 6.76 (s, 1H, Ar-*H*), 6.83 (s, 1H, Ar-*H*). ^{13}C NMR $\{^1\text{H}\}$ (75 MHz, C_6D_6): δ 18.55, 18.66, 21.06, 43.52, 69.64, 107.42, 122.88, 129.33, 129.38, 135.93, 135.96, 136.53, 138.78, 186.19. IR (KBr): 3166(m), 3140(m), 3075(w), 2916(s), 2855(m), 1487(s), 1398(s), 1330(s), 1268(m), 1230(m), 1076(w), 1038(m), 927(m), 900(m), 851(s), 741(m), 705(m). HRMS (EI) m/z : (M) $^+$ calcd, 438.1362; obsd, 438.1367.

Allyl(IrBu)NiCl (1d). Ni(cod) $_2$ (125 mg, 0.46 mmol) was suspended in cod (ca. 750 mg) in a scintillation vial. Allyl chloride (35 mg, 0.46 mmol) was then added dropwise to this suspension while the vial was swirled. A solution of IrBu (82 mg, 0.46 mmol) in toluene (2 mL) was added. The IrBu was then rinsed with toluene (2×1 mL). The vial was swirled by hand until the mixture became homogeneous (ca. 3 min). The reaction mixture was then concentrated to dryness under a vacuum to yield the product as an orange solid (144 mg, >99% yield). The product has ^1H NMR data identical to the literature values.¹² Crystals suitable for X-ray analysis were obtained by cooling a solution of **1d** in 1:1 toluene:hexanes to -25°C .

Allyl(IAd)NiCl (1e). Ni(cod) $_2$ (138 mg, 0.50 mmol) was suspended in cod (ca. 400 mg) in a scintillation vial. Allyl chloride (38 mg, 0.50 mmol) was then added dropwise to this suspension while the vial was swirled. A solution of IAd (168 mg, 0.50 mmol) in toluene (2 mL) was then added. The IAd was rinsed with toluene (2×1 mL). The vial was swirled by hand until the mixture became homogeneous (ca. 5 min). The reaction mixture was then concentrated to dryness under a vacuum to yield the product as an orange solid (233 mg, 98% yield). The product has ^1H NMR data identical to the literature values.¹²

Allyl(IBioxMe $_4$)NiCl (1f). IBioxMe $_4$ -HOTf (112 mg, 0.33 mmol) and KO t Bu (39 mg, 0.34 mmol) were dissolved in thf (3 mL) in a scintillation vial and stirred for 2 h. Benzene (2 mL) was then added to the resulting solution to precipitate KOTf. Ni(cod) $_2$ (90 mg, 0.33 mmol) was suspended in 1,5-cod (ca. 400 mg) in a second scintillation vial. Allyl chloride (26 mg, 0.34 mmol) was added to the suspension of Ni(cod) $_2$, resulting in a color change from yellow to red. The thf/benzene mixture containing IBioxMe $_4$ was then pipet-filtered over Celite directly into the Ni/allyl chloride/1,5-cod mixture, followed by 2×1 mL rinses with benzene. The resulting orange solution was concentrated to dryness under a vacuum to yield a brown solid. The complex was then dissolved in thf (3 mL), filtered over Celite into a scintillation vial, layered with hexane (10 mL), and cooled to -25°C to yield brown prisms (83 mg, 74%). Crystals suitable for X-ray analysis were obtained by cooling a solution of **1f** in 1:2 toluene:hexanes to -25°C .

^1H NMR (300 MHz, d_8 -thf): δ 1.58–1.72 (m, 7H, overlapping allyl-*H* and CR $_3$ Me), 1.87 (s, 3H, CR $_3$ Me), 2.00 (s, 3H, CR $_3$ Me), 2.39 (d, $J = 6.3$ Hz, 1H, allyl-*H*), 2.66 (d, $J = 14$ Hz, 1H, allyl-*H*), 3.30 (d, $J = 6.6$ Hz, 1H, allyl-*H*), 4.51 (dt, $J = 24$ Hz, 8.2 Hz, 4H, ROCH $_2$ CR $_2$ N), 5.24 (sept, $J = 6.6$ Hz, 1H, allyl-*H*). ^{13}C NMR $\{^1\text{H}\}$ (75 MHz, d_8 -thf): δ 25.85, 26.61, 26.67, 44.80, 61.57, 62.06, 68.38, 88.43, 88.57, 108.01, 126.94, 159.37. IR (KBr): 2964(m),

2922(m), 1748(s), 1458(s), 1411(s), 1335(s), 1255(m), 1208(s), 996(s), 935(s), 849(m), 668(w), 494(w) cm^{-1} . HRMS (EI) m/z : (M) $^+$ calcd, 342.0655; obsd, 342.0650.

Allyl(ICy)NiCl (1g). ICy-HBF $_4$ (106 mg, 0.33 mmol), KO t Bu (39 mg, 0.35 mmol), and thf (5-mL) were added to a scintillation vial, and the resulting mixture was stirred for 1 h. The mixture was diluted with toluene (2 mL) and concentrated under a vacuum to ca. 2 mL. The reaction mixture was then diluted with toluene (1 mL) and hexanes (7 mL), mixed by pipet for ca. 2 min, and filtered over Celite. The solids were washed with hexanes (2×1 mL). The filtrate was combined and concentrated to ca. 1 mL under a vacuum. Ni(cod) $_2$ (91 mg, 0.33 mmol) and cod (~400 mg) were added to a 20 mL scintillation vial. Allyl chloride (25 mg, 0.33 mmol) was then added dropwise to the resulting suspension of Ni(cod) $_2$, resulting in the appearance of a red color. After the vial was swirled until all of the solid Ni(cod) $_2$ disappeared (~5 min), the solution of ICy in toluene was added dropwise to the nickel/cod/allyl chloride mixture; residual ICy was rinsed with toluene (2×1 mL). This resulted in the formation of a brown heterogeneous mixture, which was filtered over Celite to remove a green solid. The filtrate was diluted with hexanes (9 mL) and cooled to -25°C overnight. An orange-brown precipitate formed and was isolated by pipeting off the solvent and drying the solid under a vacuum to yield the product (62 mg, 51% yield).

^1H NMR (300 MHz, C_6D_6): δ 0.8–1.0 (m, 2H, cy-*H*), 1.0–2.0 (m, 17H, cy-*H*), 1.87 (m, 1H, cy-*H*), 2.30 (m, 2H, cy-*H*), 2.61 (d, $J = 10$ Hz, 1H, allyl-*H*), 3.01 (d, $J = 14$ Hz, 1H, allyl-*H*), 3.82 (d, $J = 7.6$ Hz, 1H, allyl-*H*), 4.76 (br s, 1H, NCHR $_2$), 5.18 (sept, $J = 6.7$ Hz, 1H, allyl-*H*), 5.56 (br s, 1H, NCHR $_2$), 6.34 (s, 1H, RNCHCHNR), 6.41 (s, 1H, RNCHCHNR). ^{13}C NMR $\{^1\text{H}\}$ (75 MHz, C_6D_6): δ 25.50, 25.55, 25.59, 25.67, 25.91, 34.08, 34.24, 34.43, 42.69, 59.80, 60.39, 68.50, 107.24, 117.51, 180.84. IR (KBr): 2931(s), 2852(s), 1450(m), 1422(m), 1380(m), 1238(m), 1201(s), 895(w), 866(w), 724(s), 699(m), 424(m), 409(w) cm^{-1} . HRMS (EI) m/z : (M) $^+$ calcd, 366.1403; obsd, 366.1388.

Allyl(ITol)NiCl (1h). Ni(cod) $_2$ (171 mg, 0.62 mmol) was suspended in cod (ca. 1 g) in a scintillation vial. Allyl chloride (48 mg, 0.62 mmol) was then added dropwise to this suspension while the vial was swirled. A mixture of ITol (154 mg, 0.62 mmol) in toluene (3 mL) was then added. The ITol was then rinsed over with toluene (4×1 mL). The mixture was swirled for ca. 5 min and then concentrated under a vacuum. The product was then crystallized from toluene/hexanes at -25°C to yield an orange solid (149 mg, 63% yield).

^1H NMR (300 MHz, C_6D_6): δ 1.10 (d, $J = 12$ Hz, 1H, allyl-*H*), 1.89 (dt, $J = 6.8$ Hz, 2.4 Hz, 1H, allyl-*H*), 2.05 (s, 6H, Ar-*Me*), 2.80 (d, $J = 14$ Hz, 1H, allyl-*H*), 3.70 (dd, $J = 2.4$ Hz, 7.6 Hz, 1H, allyl-*H*), 4.76 (sept, $J = 6.8$ Hz, 1H, allyl-*H*), 6.54 (br s, 1H, RNCHCHNR), 6.61 (br s, 1H, RNCHCHNR), 6.96 (d, $J = 7.8$ Hz, 2H, Ar-*H*), 7.02 (d, $J = 7.8$ Hz, 2H, Ar-*H*), 8.01 (d, $J = 7.8$ Hz, 2H, Ar-*H*), 8.44 (d, $J = 7.6$ Hz, 2H, Ar-*H*). ^{13}C NMR $\{^1\text{H}\}$ (75 MHz, C_6D_6): δ 20.89, 43.03, 68.23, 107.49, 121.85, 122.14, 124.51, 124.85, 127.81, 127.87, 129.98, 130.03, 137.79, 138.06, 185.22. IR (KBr): 3173(w), 3140(m), 3110(w), 3054(m), 3033(m), 2918(m), 1514(s), 1409(s), 1338(m), 1273(s), 942(m), 888(m), 821(s), 717(m), 682(m) cm^{-1} ; Anal. Calcd for C $_{20}$ H $_{21}$ ClNi $_2$: Ni: C, 62.63; H, 5.52; N, 7.30. Found: C, 62.43; H, 5.69; N, 7.37.

Me t Bu-HI. 1-*t*-Butyl-1H-imidazole³⁰ (544 mg, 4.4 mmol) was added to a 25 mL round-bottomed flask equipped with a stirbar and dissolved in thf (5 mL). Iodomethane (301 μL , 4.8 mmol) was added to this solution, and the reaction mixture was stirred

(30) Liu, J.; Chen, J.; Zhao, J.; Zhao, Y.; Li, L.; Zhang, H. *Synthesis* **2003**, 2661–2666.

magnetically for 2 h. The reaction mixture was then diluted with ether (10 mL). The mixture was filtered over a medium frit. The filtrate was then purified by recrystallization from acetonitrile/ether by vapor diffusion to yield the product as white needles (566 mg, 49%).

¹H NMR (300 MHz, *d*₆-DMSO): δ 1.58 (s, 9H, *CMe*₃), 3.84 (s, 3H, N-CH₃), 7.76 (d, *J* = 1.6 Hz, 1H, RNCHCHNR), 7.99 (d, *J* = 1.8 Hz, 1H, RNCHCHNR), 9.24 (s, 1H, RNCHNR). ¹³C NMR {¹H} (75 MHz, *d*₆-DMSO): δ 29.01, 35.74, 59.29, 120.05, 123.74, 135.00; MS (EI) *m/z*: (M)⁺ calcd, 139; obsd, 139.

Allyl(MeI*Pr*)NiCl (1i). MeI*Pr*-HI (88 mg, 0.33 mmol), potassium *t*-butoxide (39 mg, 0.33 mmol), and thf (4 mL) were added to a scintillation vial. The resulting suspension was stirred for 3 h and then diluted with toluene (4 mL). The volume of the mixture was reduced to ca. 3 mL under a vacuum. Hexanes (8 mL) were added to the reaction mixture, which was then filtered over Celite. The solids were washed with hexanes (3 × 1 mL), and the combined filtrate was concentrated to ca. 1 mL under a vacuum. Ni(cod)₂ (91 mg, 0.33 mmol) was suspended in 1,5-cod (ca. 400 mg) in a second 20 mL scintillation vial. Allyl chloride (25 mg, 0.33 mmol) was added to the suspension of Ni(cod)₂, resulting in a color change from yellow to red. The solution of MeI*Pr* in toluene was then added dropwise to the Ni/allyl chloride/cod mixture with rapid mixing. The residual MeI*Pr* was transferred with toluene rinses (2 × 1 mL). After ca. 5 min, the reaction mixture was filtered over Celite and concentrated to 2 mL under a vacuum. The solution was then diluted with hexanes (8 mL) and cooled to -25 °C overnight to yield the product as an orange solid (51 mg, 56% yield). Note: this compound exists as a 3:2 mixture of atropisomers, as determined by NMR.

¹H NMR (300 MHz, CD₂Cl₂): δ 1.45 (br d, *J* = 12 Hz, 0.4H, allyl-*H*), 1.77 (s, 4.2H, superimposed *CMe*₃ and allyl-*H*), 2.05 (s, 3.6H, *CMe*₃), 2.36 (dt, *J* = 6.7 Hz, 2.5 Hz, 0.6H, allyl-*H*), 2.49 (dt, *J* = 6.8 Hz, 2.6 Hz, 0.4H, allyl-*H*), 2.69 (d, *J* = 14 Hz, 0.6H, allyl-*H*), 2.71 (d, *J* = 14 Hz, 0.4H, allyl-*H*), 3.33 (d, *J* = 2.6 Hz, 0.4H, allyl-*H*), 3.36 (d, *J* = 2.3 Hz, 0.6H, allyl-*H*), 3.95 (s, 1.2H, *NMe*), 4.40 (s, 1.8H, *NMe*), 5.16 (sept, *J* = 6.8 Hz, 0.6H, allyl-*H*), 5.48 (sept, *J* = 6.8 Hz, 0.4H, allyl-*H*), 6.88 (d, *J* = 2.2 Hz, 0.4H, RNCHCHNR), 6.98 (d, *J* = 1.9 Hz, 0.6H, RNCHCHNR), 7.04 (d, *J* = 1.9 Hz, 0.6H, RNCHCHNR), 7.10 (d, *J* = 2.1 Hz, 0.4H, RNCHCHNR). ¹³C NMR {¹H} (75 MHz, C₆D₆): δ 31.28, 31.54, 37.58, 38.27, 42.82, 42.94, 57.28, 57.67, 66.57, 66.67, 105.90, 107.05, 118.42, 118.66, 121.52, 121.63. IR (KBr): 3161(m), 3107-(s), 3053(w), 2978(s), 2937(s), 2872(w), 1610(m), 1574(m), 1468-(s), 1442(s), 1399(s), 1383(s), 1372(s), 1310(m), 1240(s), 1213(s), 1082(m), 921(w), 870(m), 758(s), 713(w), 688(m), 415(w) cm⁻¹. MS (EI) *m/z*: (M)⁺ calcd, 272.1; obsd, 272.1.

MeI*Pr*-HI. 1-(2,6-Diisopropylphenyl)-1*H*-imidazole^{30,31} (1.14 g, 5 mmol) was added to a 20 mL scintillation vial equipped with a stirbar and dissolved in thf (5 mL). Iodomethane (342 μ L, 5.5 mmol) was added to this solution, and the reaction mixture was allowed to stir for 15 h. The reaction mixture was then diluted with ether (10 mL). The crude product partitioned from the ether phase as a viscous oil. The ether layer was removed via decantation. The viscous oil was then dissolved in methylene chloride (4 mL). The addition of ether (12 mL) to this solution resulted in the precipitation of a yellow solid. The solid was isolated via filtration with a medium frit and purified via recrystallization from acetonitrile/ether by vapor diffusion to obtain the product as clear blocks (1.11 g, 60%).

¹H NMR (300 MHz, CD₂Cl₂): δ 1.16 (d, *J* = 6.8 Hz, 6H, CHMe₂), 1.25 (d, *J* = 6.8 Hz, 6H, CHMe₂), 2.34 (sept, *J* = 6.8

Hz, 2H, RCHMe₂), 4.36 (s, 3H, N-CH₃), 7.22 (t, *J* = 1.8 Hz, 1H, RNCHCHNR), 7.36 (d, *J* = 7.8 Hz, 2H, Ar-*H*), 7.59 (t, *J* = 7.8 Hz, 1H, Ar-*H*), 7.66 (br s, 1H, RNCHCHNR), 9.99 (s, 1H, RNCHNR). ¹³C NMR {¹H} (75 MHz, CD₂Cl₂): δ 24.55, 24.66, 29.09, 38.22, 124.80, 125.01, 125.17, 130.41, 132.40, 138.15, 145.94; MS (EI) *m/z*: (M)⁺ calcd, 243; obsd, 243.

Allyl(MeI*Pr*)NiCl (1j). MeI*Pr*-HI (122 mg, 0.33 mmol), potassium *t*-butoxide (39 mg, 0.33 mmol), and thf (4 mL) were added to a scintillation vial. The resulting suspension was stirred for 3 h and then diluted with toluene (4 mL). The volume of the mixture was reduced to ca. 3 mL under a vacuum. Hexanes (8 mL) were added to the reaction mixture, which was then filtered over Celite. The solids were washed with hexanes (3 × 1 mL), and the combined filtrate was concentrated to ca. 1 mL under a vacuum. Ni(cod)₂ (90 mg, 0.33 mmol) was suspended in 1,5-cod (ca. 400 mg) in a second scintillation vial. Allyl chloride (26 mg, 0.34 mmol) was added to the suspension of Ni(cod)₂, resulting in a color change from yellow to red. The solution of MeI*Pr* in toluene was then added to the Ni/allyl chloride/cod mixture by pipet with rapid mixing. Residual MeI*Pr* was transferred by pipet using additional toluene (2 × 1 mL). The reaction mixture became brown with the formation of a green precipitate. The mixture was filtered over Celite, and the precipitate was washed with hexanes (2 × 1 mL). The filtrate was concentrated to ca. 1 mL under a vacuum, diluted with hexanes (8 mL), and cooled to -25 °C overnight to precipitate the product as an orange solid (58 mg, 47% yield).

¹H NMR (300 MHz, C₆D₆): δ 0.92 (d, *J* = 6.8 Hz, 3H, CHMe₂), 0.98 (d, *J* = 6.8 Hz, 3H, CHMe₂), 1.11 (d, *J* = 13 Hz, 1H, allyl-*H*), 1.25 (d, *J* = 6.8 Hz, 3H, CHMe₂), 1.48 (d, *J* = 6.3 Hz, 3H, CHMe₂), 2.16 (d, *J* = 6.1 Hz, 1H, allyl-*H*), 2.65–2.70 (m, 2H, superimposed allyl-*H* and ArCHMe₂), 3.25 (br s, 1H, ArCHMe₂), 3.65 (d, *J* = 6.1 Hz, 1H, allyl-*H*), 3.75 (s, 3H, *NMe*), 4.77 (sept, *J* = 6.7 Hz, 1H, allyl-*H*), 6.10 (d, *J* = 4.6 Hz, 1H, RNCHCHNR), 6.33 (s, 1H, RNCHCHNR), 7.05 (d, *J* = 6.8 Hz, 1H, Ar-*H*), 7.15–7.22 (m, 2H, Ar-*H*). ¹³C NMR {¹H} (75 MHz, C₆D₆): δ 23.23, 23.69, 26.71, 26.80, 28.65, 28.84, 38.37, 43.50, 69.75, 108.29, 122.32, 124.25, 124.58, 130.48, 136.66, 146.87, 147.48, 185.39. IR (KBr): 3160(m), 3126(m), 3097(m), 2964(s), 2864(w), 1461-(s), 1399(s), 1387(m), 1360(m), 1285(m), 1218(m), 806(m), 766-(m), 734(m), 694(w), 470(w), 437(w), 423(w) cm⁻¹. HRMS (EI) *m/z*: (M)⁺ calcd, 376.1214; obsd, 376.1215.

Allyl(IME)NiCl (1k). IMe-HI (123 mg, 0.55 mmol) and KO*t*Bu (62 mg, 0.55 mmol) were added to a 20 mL scintillation vial and suspended in thf (5 mL). The resulting mixture was stirred magnetically for 4 h. The mixture was then filtered over Celite into a second vial, rinsed with thf (2 × 1 mL), and cooled to -25 °C in the glovebox refrigerator. Bis-allylnickel chloride (68 mg, 0.25 mmol) was added to a 20 mL scintillation vial and dissolved in thf (2 mL). The resulting red solution was cooled to -25 °C in the glovebox refrigerator. When both solutions were cold, the solution of IMe was added to the solution of bis-allylnickel chloride at a rate of about 1 drop per 2 s with rapid swirling of the bis-allylnickel chloride solution. A green solid rapidly precipitated from solution. The reaction mixture was mixed by hand for ca. 5 min after the addition of IMe/thf was completed. The green solid was filtered off over Celite and the filtrate was concentrated under a vacuum, resulting in the precipitation of additional green solid. The green solid was extracted with toluene (3 × 3 mL) and the toluene extracts were filtered over Celite. The toluene filtrate was then concentrated to ca. 2 mL, diluted with hexanes (8 mL), and cooled to -25 °C to precipitate a mixture of green solid and orange solid. The solid was isolated by filtration over Celite and then washed

(31) Perry, M. C.; Cui, X.; Powell, M. T.; Hou, D.-R.; Reibenspies, J. H.; Burgess, K. *J. Am. Chem. Soc.* **2003**, *125*, 113–123.

with toluene (3×2 mL). The toluene filtrate was concentrated under a vacuum to yield the product as an orange solid (61 mg, 53% yield).

^1H NMR (300 MHz, C_6D_6): δ 1.43 (d, $J = 12.7$ Hz, 1H, allyl-*H*), 2.06 (dt, $J = 6.6$ Hz, 2.4 Hz, 1H, allyl-*H*), 2.94 (d, $J = 14.2$ Hz, 1H, allyl-*H*), 3.33 (s, 6H, *NMe*), 3.83 (dd, $J = 7.6$ Hz, 2.1 Hz, 1H, allyl-*H*), 5.04 (sept, $J = 6.9$ Hz, 1H, allyl-*H*), 5.84 (s, 2H, RNCHCHNR). ^{13}C NMR $\{^1\text{H}\}$ (75 MHz, C_6D_6): δ 14.70, 37.24, 42.65, 69.08, 108.06, 121.94; IR(KBr): 3120(m), 3066(w), 2928-(w), 1571(w), 1461(m), 1400(s), 1229(s), 1196(w), 1135(w), 1088-(w), 1013(m), 919(m), (871(m), 747(s), 679(m), 568(w), 525(w), 463(m), 434(w) cm^{-1} . HRMS (EI) m/z : (M) $^+$ calcd, 230.0118; obsd, 230.0119.

Allyl(MeIrBu)NiI (11). MeIrBu-HI (133 mg, 0.5 mmol) and KOtBu (59 mg, 0.52 mmol) were added to a 20 mL scintillation vial and suspended in thf (ca. 4 mL). The resulting mixture was stirred magnetically for 90 min. In a separate 20 mL vial, Ni(cod) $_2$ (137 mg, 0.5 mmol) was suspended in 1,5-cod (ca 500 mg). To this suspension was added allyl chloride (37 mg, 0.5 mmol). The suspension of Ni(cod) $_2$ was then swirled by hand until no crystals of Ni(cod) $_2$ were visible in the vial. The reaction mixture containing MeIrBu, KI, and *t*BuOH in thf was then added to the vial containing π -allylnickel chloride by pipet. Residual material was transferred using 2×1 mL portions of thf. After ca. 5 min, the reaction mixture was filtered over Celite and concentrated to dryness under a vacuum. The product was then purified by dissolving the residue in a minimal volume of toluene (ca. 3 mL), layering the resulting solution with 10 mL hexanes, and cooling the solution to -25°C . Dark orange crystals were then isolated by pipeting off the mother liquor and drying the product under a vacuum to yield **11** (60 mg, 33% yield). One of these crystals of **11** was used for single-crystal X-ray diffraction studies. Note: this compound exists as a 2:1 mixture of atropisomers as determined by ^1H NMR.

^1H NMR (300 MHz, CD_2Cl_2): δ 1.73 (s, 6H, *CMe* $_3$), 1.98 (s, 3H, *CMe* $_3$), 2.38 (d, $J = 13.9$ Hz, 0.66H, allyl-*H*), 2.41 (d, $J = 14.2$ Hz, 0.33H, allyl-*H*), 2.94 (dt, $J = 6.8$ Hz, 2.4 Hz, 0.66H, allyl-*H*), 3.03 (dt, $J = 6.9$ Hz, 2.4 Hz, 0.33H, allyl-*H*), 3.44 (d, $J = 12$ Hz, 0.66H, allyl-*H*), 3.56 (d, $J = 7.6$ Hz, 0.33H, allyl-*H*), 3.87 (s, 1H, *NMe*), 4.23 (s, 2H, *NMe*), 4.99 (sept, $J = 6.8$ Hz, 0.66H, allyl-*H*), 5.21–5.37 (superimposed with solvent), 6.90 (d, $J = 1.9$ Hz, 0.33H, RNCHCHNR), 6.99 (d, $J = 1.9$ Hz, 0.66H, RNCHCHNR), 7.07 (d, $J = 1.9$ Hz, 0.66H, RNCHCHNR), 7.12 (d, $J = 2.0$ Hz, 0.33H, RNCHCHNR). ^{13}C NMR $\{^1\text{H}\}$ (75 MHz, C_6D_6): δ 31.46, 31.69, 38.42, 39.19, 51.06, 51.37, 63.21, 63.33, 104.74, 106.53, 119.70, 119.79, 122.58, 122.67. IR (KBr): 2979-(s), 2944(m), 2924(m), 1471(s), 1455(m), 1445(m), 1397(s), 1385-(s), 1371(s), 1306(m), 1235(s), 1210(s), 1084(m), 1017(w), 915(m), 880(w), 733(s), 687(m) cm^{-1} . Anal. Calcd for $\text{C}_{11}\text{H}_{19}\text{IN}_2\text{Ni}$: C, 36.21; H, 5.25; N, 7.68. Found: C, 36.93; H, 5.10; N, 7.65.

trans-(ITol) $_2$ NiCl $_2$ (3h). ITol complex **1h** (69 mg, 0.18 mmol) was dissolved in benzene (9 mL) in a 20 mL scintillation vial. This vial was left standing on the lab bench for 10 days. During this time, a significant quantity of fine beige powder precipitated from solution, beginning within the first day. Over the last 2 days, compact ruby red crystals of complex **3h** formed. The beige powder and mother liquor were removed via pipet. The remainder of the beige powder was removed by successive washings with hexanes (8×2 mL), although the beige solid is not soluble. Complex **3h** was then dried under a vacuum to yield red crystals suitable for X-ray analysis (12 mg, 21% yield based on ITol). Complex **3h** was insufficiently soluble in noncoordinating NMR solvents to obtain acceptable NMR spectra. Complex **3h** decomposed in coordinating NMR solvents.

IR (KBr): 3141(w), 3133(w), 3048(w), 2919(w), 1515(s), 1475-(s), 1339(m), 1279(s), 1110(w), 1089(w), 1023(w), 945(m), 841-(m), 828(m), 819(s), 730(s), 702(s), 563(m), 529(s) cm^{-1} . Anal. Calcd for $\text{C}_{34}\text{H}_{32}\text{Cl}_2\text{N}_4\text{Ni}$: C, 65.21; H, 5.15; N, 8.95. Found: C, 64.85; H, 4.86; N, 8.58.

Dynamic NMR. All VT-NMR experiments were performed on a Varian VXR-300 instrument. Values of ΔG^\ddagger were determined at coalescence for complexes **1g** and **1h** in both benzene and thf. The ΔG^\ddagger value for complex **1f** in benzene was determined below the coalescence point at temperatures between 55 and 80°C . Insufficient line-broadening was observed below 62°C for complex **1f** in thf.

Oxidation Studies. C_6D_6 : An NMR sample of each complex in d_6 -benzene in a 5 mm thin-walled NMR tube was placed under a gentle stream of O_2 that was dried via passage through a drying tube. The O_2 -reactive complexes (**1b**, **1c**, **1f**, **1j**, **1k**) rapidly changed in color with complete consumption of the starting material. The O_2 -inert (**1d**, **1e**, **1i**) complexes exhibited no change, as verified by ^1H NMR, even when heated to 80°C under O_2 . The intermediate complexes (**1f**, **1g**, **1h**, **1i**) gradually disappeared.

THF: A sample of each complex **1a–1i** (1–2.5 mg) was placed in a separate 1 dram vial. Each sample was dissolved in thf (ca. 2 mL). The resulting solutions were sparged with O_2 , capped, and allowed to stand on the bench for observation. Complexes **1a**, **1b**, **1c**, **1f**, **1g**, and **1j** immediately changed color from orange to purple upon the addition of O_2 . IMe complex **1k** immediately became yellow upon the addition of O_2 . ITol complex **1h** gradually turned purple over ~ 30 min. MeIrBu complex **1i** was completely consumed within 90 s. IrBu complex **1d** and IAd complex **1e** did not turn purple within 24 h, but were observed to decompose over 48 h, still without any observable bis- μ -hydroxonickel complex formation.

CH_2Cl_2 : A procedure similar to that for thf was used, substituting freshly distilled CH_2Cl_2 for thf. In this case, the only sample to exhibit any change in less than 5 h was IMe complex **1k**, which became yellow over 1 h with precipitation of a white solid. The only case where formation of a purple solution was observed was for IMes complex **1c**, which took 24 h. Complexes **1a**, **1b**, **1f**, **1g**, and **1j** were all observed to decompose within 36 h, albeit without any bis- μ -hydroxonickel complex formation observed.

Visible Spectroscopy. Formation of bis- μ -hydroxonickel complexes was verified by visible spectroscopy for samples **1b**, **1c**, **1f**, **1g**, **1h**, **1i**, and **1j**. These complexes were not sufficiently stable to fully characterize. However, oxidation of **1b**, **1c**, and **1j** in toluene at 0°C revealed the extremely rapid formation of broad peaks with λ_{max} values of 492 (**1b**), 497 (**1c**), and 496 nm (**1j**). Oxidation of **1f**, **1g**, **1h**, and **1i** at 0°C in thf led to products with λ_{max} values of 488 (**1f**), 483 (**1g**), 498 (**1h**), and 497 nm (**1i**). The formation of a bis- μ -hydroxonickel complex for **1k** could not be verified at 0°C . Oxidation of **1k** at -36°C also did not reveal a peak at ~ 500 nm. In the oxidation of **1k**, the product lacks any peaks in the visible region, with only a strong UV absorbance with a wide shoulder into the visible region.

Acknowledgment. This work was supported by the University of Utah Research Foundation and partially supported by the National Institutes of Health (NIGMS RO1 GM3540).

Supporting Information Available: Crystallographic details, ^1H NMR spectra, and VT-NMR spectra. This material is available free of charge via the Internet at <http://pubs.acs.org>.

IC0612451